Polym. Bull. (2010) 64:907–923
DOI 10.1007/s00289-009-0231-z

ORIGINAL PAPER

On the magnetic, mechanical and rheological properties of rubber–nickel nanocomposites

E. Muhammad Abdul Jamal · P. A. Joy · Philip Kurian · M. R. Anantharaman

Received: 21 January 2009 / Revised: 12 May 2009 / Accepted: 17 December 2009 /
Published online: 25 December 2009

Abstract Rubber–nickel nanocomposites were synthesized by incorporating freshly prepared nanometric nickel particles in two different matrices namely natural rubber and neoprene rubber according to specific recipes for various loadings of nano nickel and the cure characteristics of these composites were evaluated. The maximum torque values register an increase with the increase in loading of nickel in both composites and this is attributed to the non-interacting nature of nickel nanoparticles with rubber matrices. The cure time of natural rubber composites decreases with increase in the content of nickel, and in neoprene rubber cure, time increases with increase in filler content. In natural rubber, the curing reaction seems to be activated by the presence of nickel particles. The magnetization studies of the composites reveal that the magnetic properties of nickel are retained in the composite samples. The elastic modulus of natural rubber and neoprene rubber are largely improved by the incorporation of nickel particles.

Keywords Nanocomposites · Cure characteristics · Elastic modulus · Magnetic properties

E. M. A. Jamal · M. R. Anantharaman (✉)
Department of Physics, Cochin University of Science and Technology, Cochin 682 022, India
e-mail: mraiyer@yahoo.com

P. A. Joy
National Chemical Laboratory, Pune, India

P. Kurian
Department of Polymer Science and Rubber Technology, Cochin University of Science and Technology, Cochin 682 022, India

Introduction

Elastomer magnetic nanocomposites find a number of technological applications like flexible magnets, electromagnetic shielders and stealth materials. This can be achieved by incorporating suitable magnetic filler in the elastomeric matrix such as iron oxides like ferrites or metallic particles like nickel or iron [1–5]. Employing metallic particles as fillers is advantageous mainly because of the requirement of only a low volume fraction of particles due to their higher density in comparison to ferrite fillers. A chemically stable metallic magnetic particle like nickel is a suitable magnetic filler candidate for the synthesis of magnetic elastomeric composites. However, normal micron-sized metal-filled magnetic composites intended for microwave applications have the disadvantage that they cannot be used in the higher frequency regime of microwaves. At higher frequencies, the magnetic permeability of the metal particle drops considerably due to skin effect, and the magnetic properties virtually become insignificant after 10 GHz [6]. However, this disadvantage can be overcome if nanometre-sized metal particles are used as fillers because the sizes of such particles are smaller than the skin depth of the electromagnetic radiations in metals [7].

For making flexible elastomeric magnetic nanocomposites, natural rubber or synthetic elastomer like neoprene rubber can be an ideal matrix. Natural rubber is an immediate choice because of its low cost and easy availability in this part of the world. Among various synthetic rubbers available, neoprene appears to be a better choice, again because of the ease in processability and other characteristics like higher resistance to flame, to weathering, to salinity and to harsh chemicals [8].

Evaluation of cure characteristics of the vulcanisates is very important as it throws light on the mechanism of interaction of the filler with the polymer. Moreover, the estimation of maximum and minimum torque indirectly provides information about the modulus and other mechanical properties. The estimation of magnetic and mechanical properties of these composites also assumes significance. It is to be ensured that the loading is uniform and has a direct bearing on the saturation magnetization of the composite. The matrix impregnated with magnetic filler not only modifies the magnetic properties, but also imparts reinforcing characteristics to the matrix. All these can be determined by evaluating the mechanical and magnetic properties of the composites.

Two types of matrix are chosen here to prepare two sets of composites: (a) natural-rubber–nickel composites (NRNCs) and (b) neoprene–nickel composites (NNCs). The cure characteristics of the composites and influence of magnetic metallic fillers on the mechanical and magnetic properties of the elastomers are investigated in this article.

Experimental details

Materials

Natural rubber and neoprene rubber were used as the matrix for the preparation of two series of composites. Compounding ingredients like sulphur, accelerators, stearic acid

Table 1 Recipes for the preparation of NRNCs and NNCs

NRNC		NNC	
Ingredients	Weight (g)	Ingredients	Weight (g)
Natural rubber	100	Synthetic rubber	100
Zinc oxide	4	MgO	4
Steiric acid	2	Stearic acid	1
CBS	1	Filler (Ni)	phr
Filler (Ni)	phr	NA22	0.5
Sulphur	2.5	ZnO	5

and zinc oxide were utilized according to specific recipes as presented in Table 1. For the synthesis of nickel nanoparticles, nickel nitrate hexahydrate and ethylene glycol were purchased from Merck, India and used without any further purification.

Synthesis of nickel particles

Nickel particles were synthesized by the authors using a modified sol–gel combustion process (patent pending—patent application No 1927/07/Indian patent) Better reduction in particle size was achieved by employing this modified process. To further reduce the size of the particles below 100 nm, the synthesized powder was subjected to high energy ball-milling using a Fritsch planetary ball mill model P-7 for around 2 h. Nickel particles used as filler are in the size range of 25 to 40 nm.

Initial characterization of nickel nanoparticles

The structural analysis of nickel particles were carried out by means of an X-ray diffractometer (XRD) (Rigaku Dmax C with Cu Kα X-ray source of wavelength of 1.54 Å). Superconducting quantum interference device magnetometry (SQUID) was employed for evaluating the magnetic properties of nickel nanoparticles (MPMS-5S XL Quantum Design magnetomer). The structural properties of the prepared nanocomposites were also analyzed using XRD.

Preparation of composites

The curing of the NRNCs and NNCs was carried out as per ASTM procedure reported elsewhere [9, 10]. The recipe used in the preparation of the samples is presented in Table 1. Six samples were prepared in each series; five samples each with content of nickel varying from 20 phr (parts per hundred rubbers by weight) to 100 phr along with a gum vulcanisate. The mixing of the elastomer along with the compounding ingredients and the nickel filler were carried out in a Brabender Plasticoder according to recipes formulated arrived by trial and error at 60 °C. The mixed material was homogenized in a two-roll mill operated with a friction ratio of 1:1.25 and the homogenized sheets were matured for 24 h before evaluating the cure characteristics. The cure times were determined for each composite sample

separately using a rubber process analyzer (RPA2000 of α-Technology). The NRNC samples were cured at a temperature 150 °C and NNC samples at 160 °C to their respective cure times in the form of sheets of thickness 2 mm using an electrically heated hydraulic press at a pressure of 140 kg cm^{-2}.

Evaluation of cure characteristics

The cure characteristics of the composites were determined using a Rubber Processing Analyzer (RPA 2000 of α-technology), by measuring torque against time at a pre-programmed strain. Different cure parameters obtained from the RPA are listed below.

- Minimum torque (D_{min}): Torque obtained by mix after homogenizing at the test temperature and before the onset of cure.
- Maximum torque (D_{max}): Maximum torque recorded at the completion of cure.
- Optimum cure time, t_{90}: This is the time taken for obtaining 90% of the maximum torque.
- Scorch time, t_{10}: It is the time taken for two unit rise above minimum torque (i.e. about 10% vulcanization).
- Cure-rate index (CRI): CRI is calculated from the following equation:

$$\text{Cure rate index} = \frac{100}{t_{90} - t_{10}}. \quad (1)$$

Mechanical, magnetic and morphological properties of composites

Mechanical properties of the composites were determined according to ASTM standards (ASTM D 412-98a (2002)) using a Shimadzu universal testing machine model SPL-10KN with the speed of the cross head fixed at 500 mm/min. The stress developed in the samples at 50, 100, 200, 300% strains along with the maximum stress (breaking stress) and the corresponding strain was measured. The hardness of the specimens were evaluated using a Shore A Durometer and resilience with a vertical rebound resilometer using cylindrical samples 16 mm in diameter and 6 mm thick. Vibrating sample magnetometry (VSM) (EG&G PAR 2000 VSM) was employed to study the magnetic properties of the composites at room temperature. Scanning electron microscopy (SEM) (JEOL model JSM–6390LV) was used to study the morphology of the composites on the fractured surfaces (obtained by doing the tensile-strength measurements on the UTM).

Results and discussion

Structural and magnetic studies of nickel particles

The X-ray diffraction pattern of nickel particles is shown in Fig. 1. The results obtained from the XRD studies were used for the analysis of structural properties of

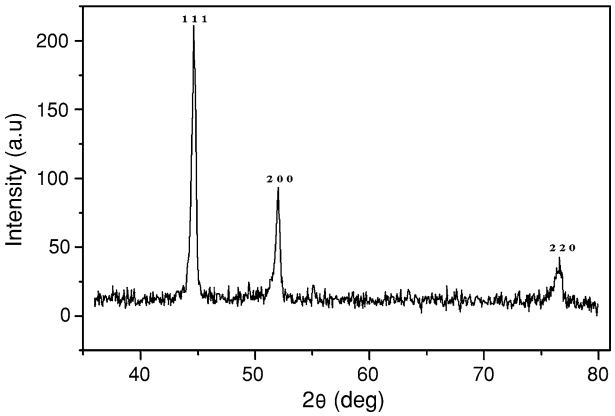

Fig. 1 XRD pattern of nickel nanoparticles

the nickel particles. The XRD pattern was compared with the published results available in ICDD (International Centre for Diffraction Data) files, and it was found that the obtained pattern exactly matches with the reported result (ICDD data file no 03-1051). The diffraction peaks were identified and indexed. Particle size, D, was determined using Debye–Scherrer formula given as:

$$D = \frac{0.9\lambda}{\beta \cos \theta}, \tag{2}$$

where λ is the wavelength of the X-ray source, β the full width at half maximum of the diffraction peaks in radians and 2θ the diffraction angle [11]. The average particle size was evaluated and found to be 26 nm. The magnetic hysteresis of nickel particles is presented in Fig. 2. The result indicates that the particles are ferromagnetic with a coercivity of 68 Oe and a remanent magnetization of 8.5 emu/g. The saturation magnetization is found to be 47.5 emu/g, and this also is about 87% of the magnetization of bulk nickel sample, which was reported elsewhere [12]. Formation of dead layer at the surface of nanoparticles could be attributed for the observed drop in saturation magnetization [13].

Cure characteristics of NRNCs

The cure-time graph of NRNCs recorded in the RPA is depicted in Fig. 3, and the cure parameters deduced from the cure-time graph are presented in Table 2. The maximum torque, which represents the shear modulus of the fully vulcanized rubber composites, increases with increase in loading of nickel. At the time of mixing due to the effect of high shearing forces, the elastomer breaks down facilitating active sites on the molecules [10]. Rubber bound nickel particles formed by the interaction with active sites on polymer molecules cause the enhancement of shear modulus of the composites. This is a clear indication that the presence of nanometre-sized nickel particles has a reinforcing effect in the natural rubber matrix. Minimum torque of the rubber compound is a measure of viscosity of the compound.

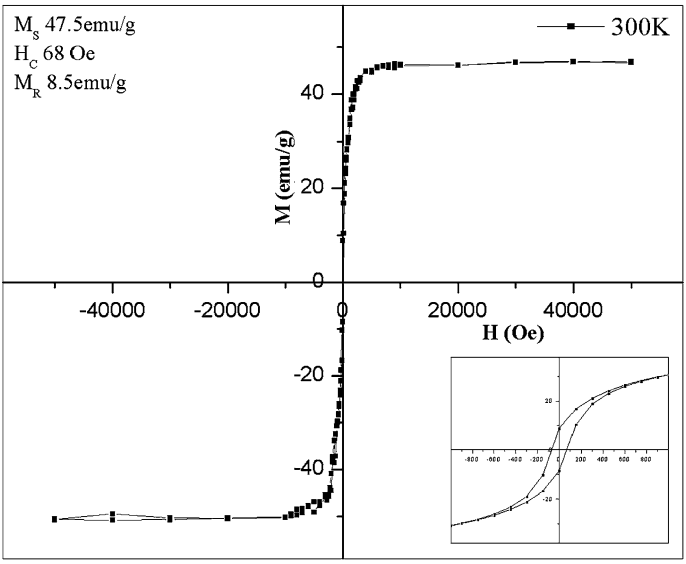

Fig. 2 Magnetic hysteresis loop of nickel particles with enlarged central region showing magnetic coercivity and remanence

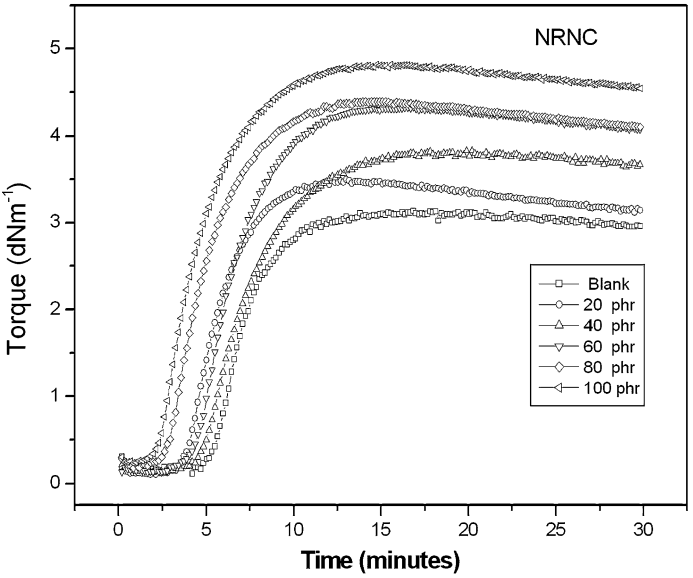

Fig. 3 Cure characteristics of NRNCs

In NRNC, the minimum torque remains almost steady up to filler loading of 60 phr and after that it registers an increase. The absence of large variations in minimum torque indicates that the processability of rubber is not hindered due to the addition

Table 2 Cure properties of NRNC samples

Filler loading (phr)	0	20	40	60	80	100
Minimum torque (dNm)	0.153	0.101	0.127	0.13	0.179	0.251
Maximum torque (dNm)	3.095	3.4	3.8	4.32	4.4	4.8
Scorch time (min)	3.82	3.53	3.16	2.85	1.91	1.62
Cure time (min)	9.3	7.83	7.39	6.32	5.47	5.2

of nickel nanoparticles. At higher filler ratios, the occlusion of rubber within and between filler aggregates may take place and causes immobility of elastomer layers resulting in an increase in minimum torque.

Torque variation in gum and filled compounds can be analyzed with the help of the expression proposed by Wolf and Westlinning [14, 15]. According to this expression, the relative torque difference between minimum and maximum torques of the gum and filled compounds is directly proportional to the filler loading. The Wolf and Westlinning equation can be written as:

$$\frac{D_{\max} - D_{\min}}{D^0_{\max} - D^0_{\min}} - 1 = \alpha_F \frac{m_f}{m_p}, \tag{3}$$

where D indicates the torques with the subscripts max and min for maximum and minimum and the superscript 0 for the blank rubber samples. The masses of filler and polymer in the compound are indicated by m_f and m_p, respectively, and α_F is a specific constant whose value can give some indications about the final state of filler in the composites. The plot of $\frac{D_{\max}-D_{\min}}{D^0_{\max}-D^0_{\min}} - 1$ against $\frac{m_f}{m_p}$ is depicted in Fig. 4. The slope of this curve gives α_F, and we have obtained a near straight line graph passing

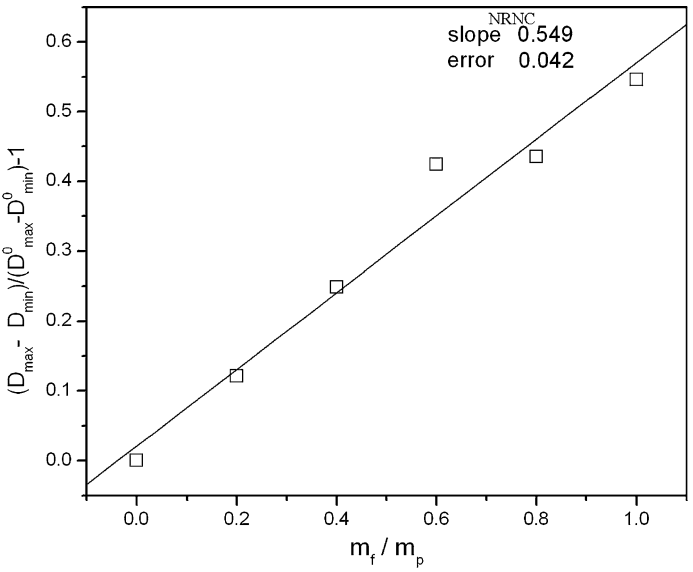

Fig. 4 The graph of $\frac{D_{\max}-D_{\min}}{D^0_{\max}-D^0_{\min}} - 1$ of NNRCs plotted against $\frac{m_f}{m_p}$. The graph is a near perfect straight line

closely through the origin and α_F is found to have an average value of 0.550 with an error of only 0.042. The variation in α_F is minimal and this indicates that the dispersion of nickel particles in the natural rubber matrix is uniform. The presence of nickel nanoparticles as filler in the natural rubber matrix does not produce any chemical interaction and the observed increase in maximum torque is purely because of physical reasons. The variation of difference in torque (Δtorque) with filler loading also is nearly linear, again a clear indication of chemically non-interacting filler in the matrix is seen. Due to low volume ratio of nickel particles owing to its high density, inter particular attachments of polymer chains may be absent at all loadings, and this can be another reason for the linear variation of torque difference with the filler loading.

The cure time of NRNC shows a steady and linear decrease with filler loading as given in Table 2. The cure time for gum compound was found to be 9.3 min and for the compound with 100 phr, the cure time decreases to 5.2 min. It was observed that even though the maximum torque increases with filler loading, the time taken to reach the maximum torque decreases sharply. Nickel is a well-known catalyst used in many organic chemical reactions [16]. The presence of fine particles of nickel appears to activate the process of cross-linking of natural rubber, and the observed decrease in cure time is due to the catalytic action of nickel particles in the curing reaction. The CRI of the NRNC compounds is depicted in Fig. 5 and shows a sharp increase initially, up to a filler loading of 60 phr and afterwards it shows a decrease. A decrease in CRI is because of the wetting of the surface of filler particles by the elastomer molecules [10]. The volume fraction of nickel particles is small as already pointed out and the wetting effect cannot produce any significant decrease in CRI in

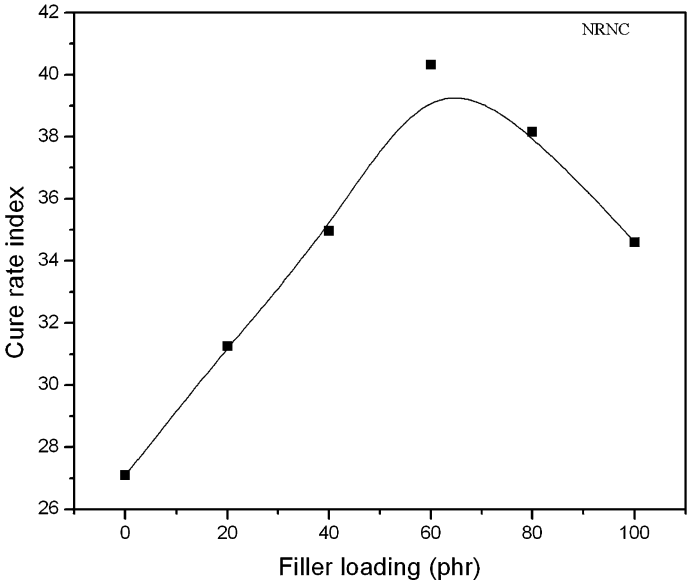

Fig. 5 Cure-rate index of NRNC samples

the initial stages. The decrease in CRI at higher filler loadings is an indication of such wetting becoming significant when the volume fraction increases. The variation of scorch time with filler loading is given in Table 2, and the decrease in scorch time is mainly due to the activation in cross-linking reaction by the presence of fine particles of nickel.

Cure characteristics of NNCs

The cure-time graph of NNCs recorded in the RPA is depicted in Fig. 6, and the cure parameters deduced from the cure-time graph are presented in Table 3. The variation of minimum torque and maximum torque of the NNC during the process of curing is shown in this table. The maximum torque increase steadily with nickel loading, and in neoprene rubber matrix, also the fine particle nickel act as a reinforcing agent. However, at 100 phr loading, maximum torque drops slightly and this may due to the effect of agglomeration at high volume fraction of filler. (In NRNCs, the effect due to agglomeration of nickel particles might have been

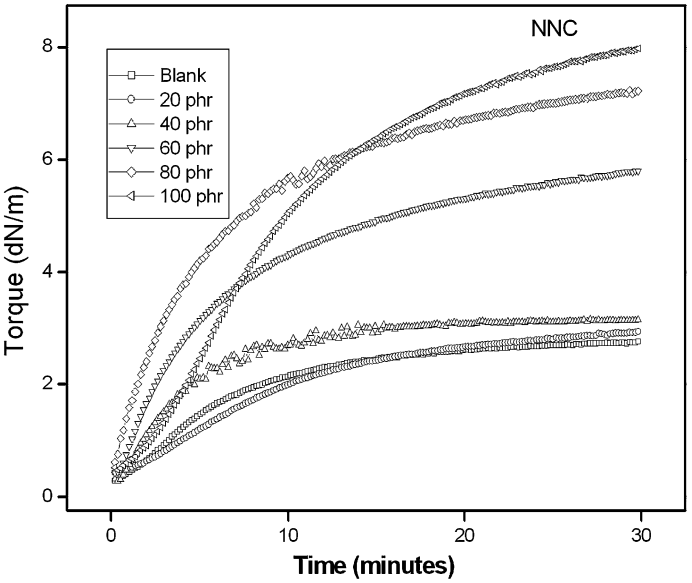

Fig. 6 Cure characteristics of NNCs

Table 3 Cure properties of NNC samples

Filler loading (phr)	0	20	40	60	80	100
Minimum torque (dNm)	0.275	0.29	0.422	0.425	0.53	0.536
Maximum torque (dNm)	3.161	4.399	4.929	5.815	7.845	7.24
Scorch time (min)	0.99	1.03	0.88	1.11	1.01	0.75
Cure time (min)	11.16	15.27	16.08	19.02	21.13	22.3

masked by the catalytic effect of nickel in the cure process, and this could be the reason for not observing any drop in maximum torque at higher loading of nickel). The minimum torque also increases with the loading of filler particles and the effect is almost similar to NRNCs. The steady increase in minimum torque can be attributed to the immobilization of elastomer chains at the surface of the filler particles.

The plot of $\frac{D_{max}-D_{min}}{D^0_{max}-D^0_{min}} - 1$ against $\frac{m_f}{m_p}$ as depicted in Fig. 7 is a straight line passing very nearly through the origin (zero). The average value of the constant α_F is 1.46 with an error of only around 0.2. The linear behaviour of the plot between $\frac{D_{max}-D_{min}}{D^0_{max}-D^0_{min}} - 1$ against $\frac{m_f}{m_p}$ is a clear indication of non-interacting filler particles. As in the case of NRNC samples, the variation of Δtorque with loading also is linear.

The variation of cure behaviour (as given in Table 3) of neoprene rubber composites is totally different from that of natural rubber composites. The cure time in NNC steadily increases with the filler content. This can be explained as follows. In NNCs, there is a steady increase in the maximum torque with the increase in filler loading. It is obvious that the cross-linking process in neoprene is not catalyzed by nickel. The maximum torque and the cure time increases almost in the same ratio since the time taken to reach maximum torque increases as there is enhancement in maximum torque. CRI of neoprene composites shows a decrease with increase in the filler content as depicted in Fig. 8. The wetting of surface of the particles is more effective in neoprene in comparison to natural rubber. The neoprene polymer chains are smaller than that of natural rubber, and this may be a reason for the enhanced wetting of particles by the polymer in the case of neoprene.

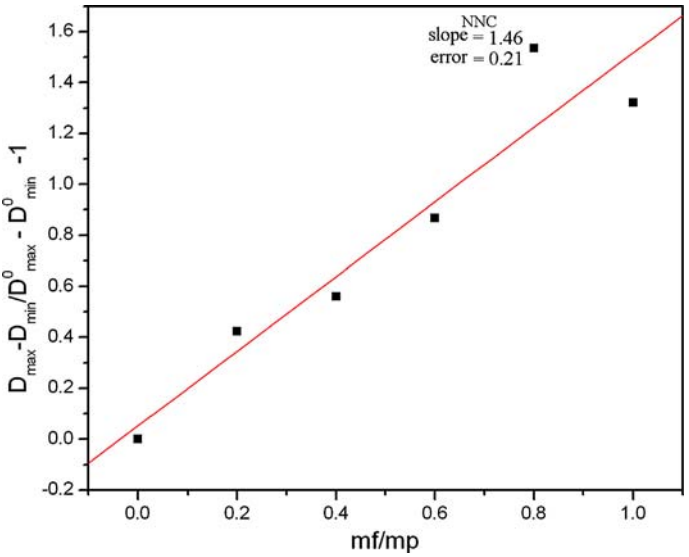

Fig. 7 The graph of $\frac{D_{max}-D_{min}}{D^0_{max}-D^0_{min}} - 1$ of NNCs plotted against $\frac{m_f}{m_p}$. The graph is a near perfect straight line

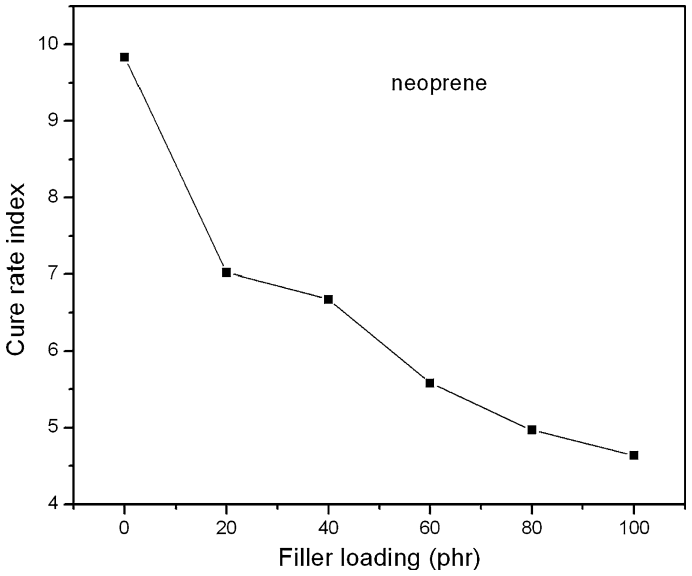

Fig. 8 Cure-rate index of NNC samples

Mechanical properties of NRNCs

Main features of the elastic properties of NRNC samples are shown in Table 4. The elastic modulus of the samples shows improvement as the nickel content in the composites increases. It can be observed that the stress developed for strains from 50 to 300% enhances as the loading increases. This is a clear indication of the reinforcing effect of nanoparticles of nickel incorporated in natural rubber matrix. However, in the case of NRNC samples, there is a steady decrease in breaking stress with the increase in filler loading. This phenomenon can be due the formation of agglomerates of filler particles inside the rubber matrix. Chances for the formation of agglomerates are higher in nickel particles compared to other metal particles because of the magnetic properties of nickel.

Table 4 Elastic properties of NRNC samples

Filler loading (phr)	Tensile strength (N/mm^2)	Elongation at break (%)	Modulus at 50% strain (N/mm^2)	Modulus at 100% strain (N/mm^2)	Modulus at 200% strain (N/mm^2)	Modulus at 300% strain (N/mm^2)
0	28.87	1210	0.3516	0.7511	1.275	1.873
20	26.65	1102	0.4168	0.7927	1.356	1.992
40	22.83	930.2	0.4703	0.9053	1.591	2.355
60	21.61	858.2	0.5497	1.0569	1.947	2.920
80	20.50	858.6	0.5851	1.1192	2.074	3.148
100	19.15	763.9	0.7898	1.3941	2.503	3.743

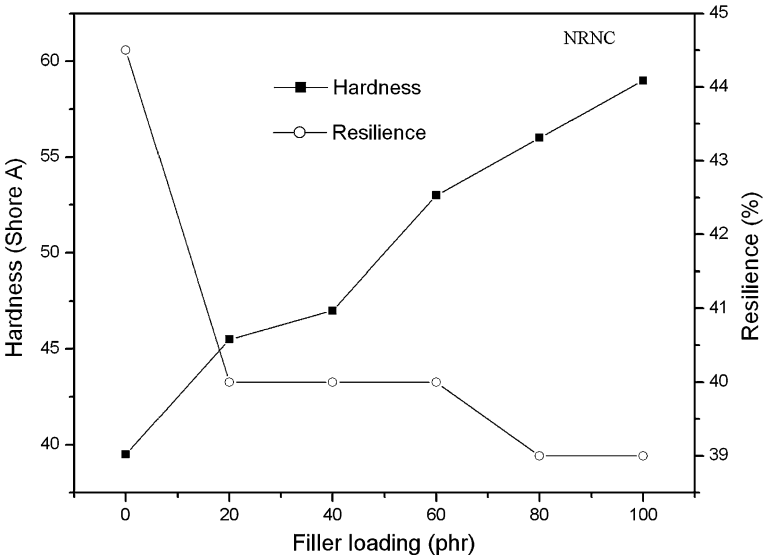

Fig. 9 Variation of hardness and resilience of NRNCs with filler loading

The variations in hardness and resilience with filler loading of NRNCs are shown in Fig. 9, and it can be observed that the hardness of the composite samples increases, whereas the resilience decreases with the increase in filler concentration. The hardness is a measure of elastic modulus at small strains. Increase in hardness is due to the drop in the mobility of the elastomer chains due to the incorporation of metal particulate filler. The decrease in resilience is due to decrease in damping property of the composite due to decrease in rubber content in the samples.

Mechanical properties of NNCs

Table 5 shows the elastic properties of NNC samples. There is considerable increase in the elastic modulus of the composites as the content of nickel increases. The stress required for a fixed strain increased steadily with the increase in filler ratio.

Table 5 Elastic properties of NNC samples

Filler loading (phr)	Tensile strength (N/mm^2)	Elongation at break (%)	Modulus at 50% strain (N/mm^2)	Modulus at 100% strain (N/mm^2)	Modulus at 200% strain (N/mm^2)	Modulus at 300% strain (N/mm^2)
0	12.32	1005.8	0.2416	0.6659	0.7327	1.208
20	12.64	932.7	0.4659	0.6207	1.115	1.461
40	12.83	918.2	0.5712	0.6102	1.282	1.761
60	11.39	847.1	0.6681	1.005	1.404	2.042
80	11.39	795.8	0.7206	0.9859	1.792	2.309
100	11.31	732.3	0.7881	1.351	2.058	2.816

The breaking stress shows an increase up to 40 phr filler concentration and thereafter exhibits a decrease. The decrease in tensile property is not as pronounced as that in NRNC samples. The reinforcing nature of the filler is evident in neoprene matrix also. Corresponding to a filler addition of 100 phr there is 225% increase in elastic modulus (at 50% strain) whereas the decrease in tensile strength is only 8%.

The hardness and resilience show similar behaviour as observed in natural-rubber-based composites and is depicted in Fig. 10. The increase in hardness can be attributed to the improvement of elastic modulus at small strains.

Magnetic properties of the composites

The magnetic properties of cured rubber samples clearly indicate that the ferromagnetic characteristics of nickel particles are retained in the NRNC and NNC samples. Figures 11 and 12 depict the magnetic hysteresis of NRNC and NNC samples, respectively. A steady increase in saturation magnetization with increase in filler fraction can be observed in both composite samples from the magnetization curves and the magnetic properties are identical in both types of composites.

The evaluation of magnetic properties of NRNCs and NNCs were carried out in similar conditions. It was observed that the coercivity of the samples did not show any variation with the concentration of nickel particles in the composites. Further the coercivity values remain nearly the same in both series of composites as depicted in Figs. 13 and 14, which are the enlarged low field region of the magnetic hysteresis loop. The reason for a small enhancement in the coercivity observed in NRNCs is not clear. However, it could be due to the higher shear modulus of natural

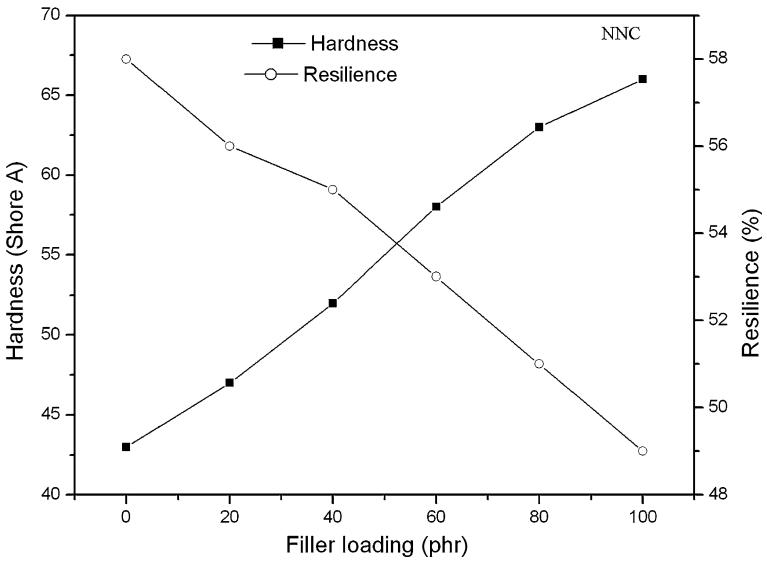

Fig. 10 Variation of hardness and resilience of NNCs with filler loading

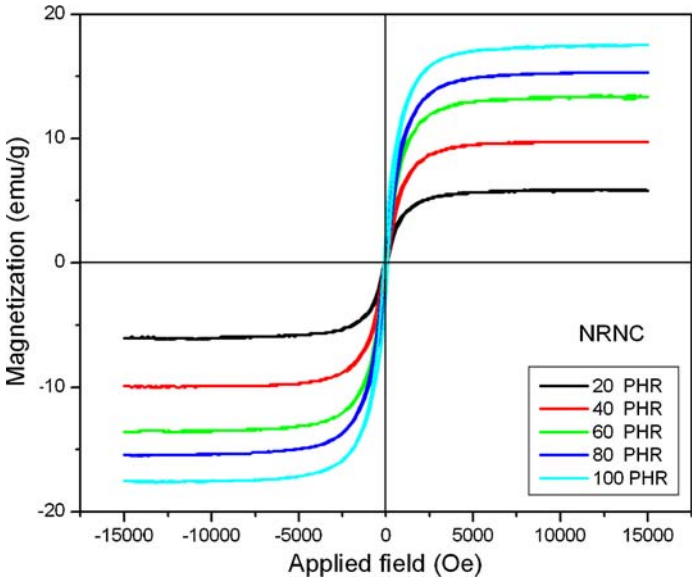

Fig. 11 Magnetic hysteresis of NRNC samples

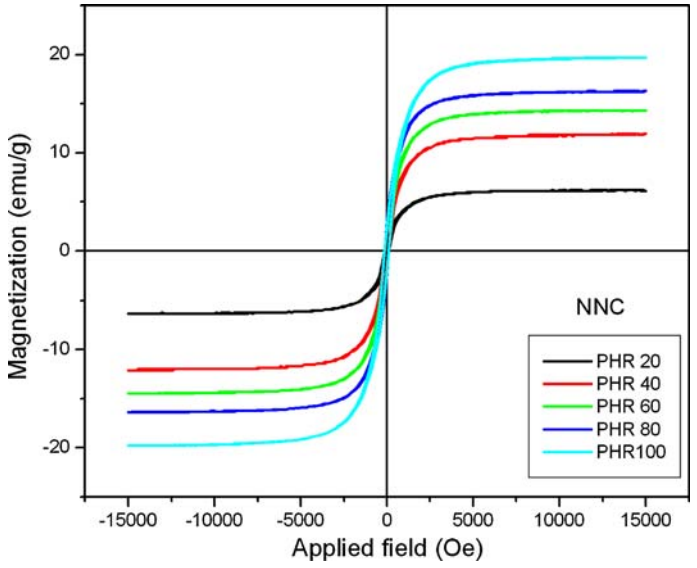

Fig. 12 Magnetic hysteresis of NNC samples

rubber compared to neoprene rubber. The remanent magnetization keeps a linear variation with the increase in concentration of nickel nanoparticle again keeping exactly the same characteristics in both composite types.

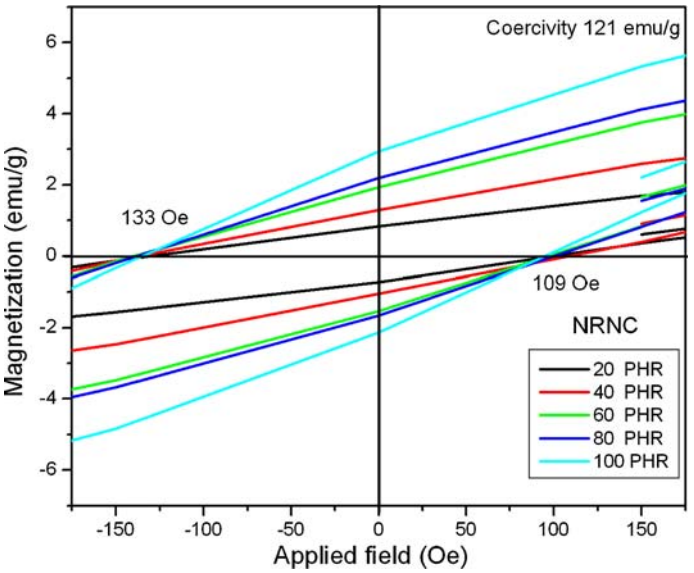

Fig. 13 Variation in remanent magnetization and coercivity of NRNC samples

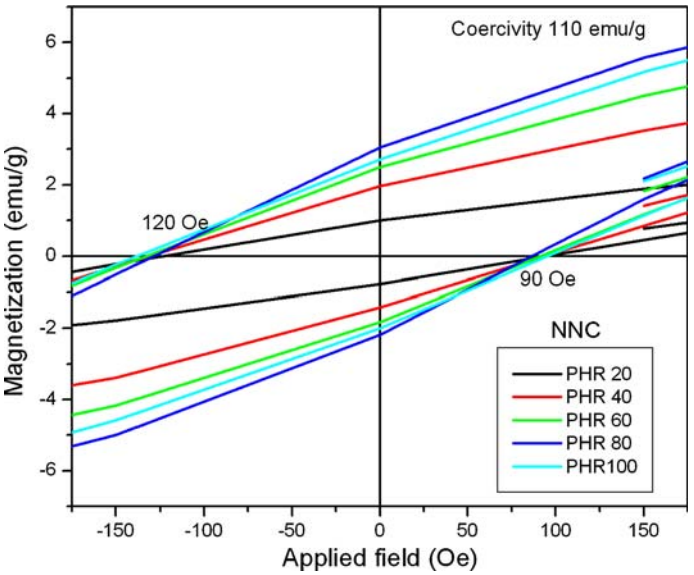

Fig. 14 Variation in remanent magnetization and coercivity of NNC samples

Morphology of the composites

Scanning electron microscopic pictures of both NRNCs and NNCs are provided as Fig. 15. Figure 15a is the SEM micrograph of natural-rubber-based composite

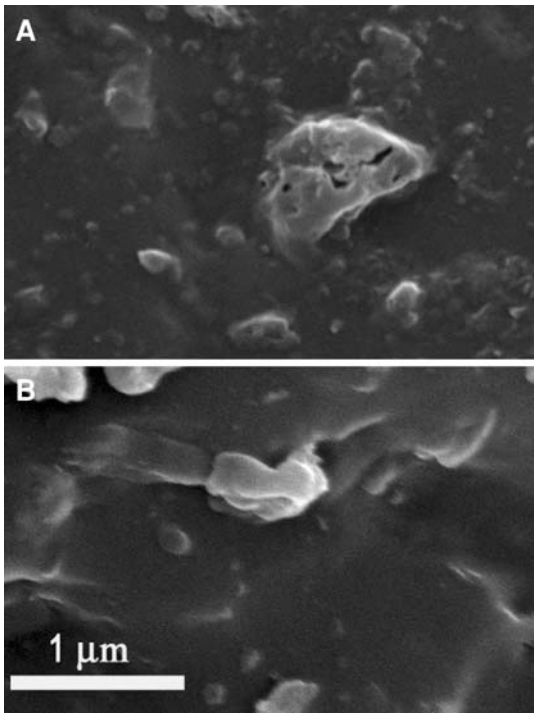

Fig. 15 : Scanning electron micrograph of the nickel-elastomer nanocomposites. **a** is that of nickel–natural-rubber composite and **b** that of nickel–neoprene-rubber composite, both at 60 phr loading

(NRNC), and Fig. 15b is that of neoprene-rubber-based composite (NNC), both at the same magnification of 20,000×. The rough topography of both the composites visible in the SEM micrographs is due the fracturing process. As the stress builds up in the matrix, the stress distribution becomes more and more non-uniform resulting in the rough topography. Sub-micron-sized nickel particles are clearly visible in both micrographs. It is quite clear that nickel particles are well dispersed in the elastomer matrices.

Conclusion

The cure characteristics of natural-rubber–nickel and neoprene–nickel nanocomposites were evaluated and the cure properties of these two series of composites were compared. There is an increase in the maximum torque values in both series of composites, and this establishes the reinforcing effect of nanoparticles of nickel in elastomeric matrices. The variation in Wolf and Westlinning constant is minimal in both the composites, and this shows that the dispersion of nickel in natural rubber and neoprene rubber matrices is uniform and filler elastomer interaction is totally absent. The presence of nickel nanoparticles in the matrices does not produce any chemical interaction, and the observed increase in maximum torque is purely due to certain physical interactions. The curing process of natural rubber appears to be catalyzed by the presence of nickel particles and such an effect is not observed in

neoprene rubber composites. Incorporation of nickel nanoparticles had improved the elastic modulus of both natural-rubber- and neoprene-based nanocomposites. The saturation magnetization and the remanence of the composites increase in a linear fashion with the concentration of nickel particles. The coercivity of the samples remains a constant in all samples in both of the series of composites. Thus, incorporation of nickel nanoparticles in matrices like natural rubber and neoprene rubber can result in magnetic nanocomposites with the required mechanical and magnetic properties. This can be achieved by tuning the loading of the fillers. Further they can also be potential materials for microwave absorbers.

References

1. Zhang B, Feng Y, Xiong J, Yang Y, Lu H (2006) Microwave-absorbing properties of de-aggregated flake-shaped carbonyl-iron particle composites at 2–18 GHz. IEEE Trans Magn 42(7):1778–1781
2. Yosoff AN, Abdullah MH, Ahmed SH, Jusoh SF, Mansor AA, Hamid SAA (2002) Electromagnetic and absorption properties of some microwave absorbers. J Appl Phys 92(2):876–882
3. He Y, Gong R, Nie Y, He H, Zhao Z (2005) Optimization of two-layer electromagnetic wave absorbers composed of magnetic and dielectric materials in gigahertz frequency band. J Appl Phys 98:084903-1–084903-5
4. Mohammed EM, Malini KA, Joy PA, Kulkarni SD, Date SK, Kurian P, Anantharaman MR (2002) Processability, hardness and magnetic properties of rubber ferrite composites containing manganese zinc ferrites. Plast Rubber Compos 31(3):106–113
5. Sindhu S, Anantharaman MR, Bindu PT, Malini KA, Kurian P (2002) Evaluation of a.c. conductivity of rubber ferrite composites from dielectric measurements. Bull Mater Sci 25(7):599–607
6. Stepan L (2008) Microwave characterization of nickel. PIERS Online 4(6):686–690
7. Chung DDL (2003) Composite materials: science and applications, functional materials for modern technologies. Springer-Verlag, London, p 93
8. Morton M (1995) Rubber technology, 3rd edn. Van Nostrand Reinold Company, New York
9. Malini KA, Kurian P, Anantharaman MR (2003) Loading dependence similarities on the cure time and mechanical properties of rubber ferrite composites containing nickel zinc ferrite. Mater Lett 57(22–23):3381–3386
10. Prema KH, Philip K, Joy PA, Anantharaman MR (2008) Physicomechanical and magnetic properties of neoprene based rubber ferrite composites. Polym Plast Technol Eng 47(2):137–146
11. Keer HV (1998) Principles of solid state physics. Wiley Eastern Ltd., New Delhi
12. Dong-Hwang C, Szu-Han W (2000) Synthesis of nickel nanoparticles in water-in-oil microemulsions. Chem Mater 12:1354–1360
13. Masala O, Seshadri R (2005) Magnetic properties of capped, soluble $MnFe_2O_4$ nanoparticles. Chem Phys Lett 402(1–3):160–164
14. da Costa HM, Visconte LLY, Nunes RCR, Furtado CRG (2004) Rice husk ash filled natural rubber compounds—the use of rheometric data to qualitatively estimate optimum filler loading. Int J Polym Mater 53:475–497
15. Wolf S (1996) Chemical aspects of rubber reinforcement by fillers. Rubber Chem Technol 69(3):325–346
16. Bonner WA, Grimm RA (1966) Nickel as an alkylation catalyst. J Org Chem 31(12):4304–4307